



HAL
open science

Estimating babassu palm density using automatic palm tree detection with very high spatial resolution satellite images

Alessio Moreira dos Santos, Danielle Mitja, Eric Delaître, Laurent Demagistri, Izildinha de Souza Miranda, Thérèse Libourel Rouge, Michel Petit

► To cite this version:

Alessio Moreira dos Santos, Danielle Mitja, Eric Delaître, Laurent Demagistri, Izildinha de Souza Miranda, et al.. Estimating babassu palm density using automatic palm tree detection with very high spatial resolution satellite images. *Journal of Environmental Management*, 2017, 193, pp.40 - 51. 10.1016/j.jenvman.2017.02.004 . ird-01715147

HAL Id: ird-01715147

<https://ird.hal.science/ird-01715147>

Submitted on 22 Feb 2018

HAL is a multi-disciplinary open access archive for the deposit and dissemination of scientific research documents, whether they are published or not. The documents may come from teaching and research institutions in France or abroad, or from public or private research centers.

L'archive ouverte pluridisciplinaire **HAL**, est destinée au dépôt et à la diffusion de documents scientifiques de niveau recherche, publiés ou non, émanant des établissements d'enseignement et de recherche français ou étrangers, des laboratoires publics ou privés.

1 **Estimating babassu palm density using automatic palm tree detection with very high**
2 **spatial resolution satellite images**

3 Alessio Moreira dos Santos ^{ab*}, Danielle Mitja^c, Eric Delaître^c, Laurent Demagistri^c, Izildinha de
4 Souza Miranda^a, Thérèse Libourel^c, Michel Petit^d.

5

6 a. Universidade Federal Rural da Amazonia (UFRA), CP.917, Belém, Pará, 66077-530, Belém,
7 Brazil. alessiomsag@gmail.com, izildinha.miranda@ufra.edu.br

8 b. Universidade Federal do Sul e Sudeste do Pará (UNIFESSPA), Folha 31, Quadra 07, Lote
9 Especial, Nova Marabá, 68507-590, Marabá, Brazil.

10 c. Institut de Recherche pour le Développement (IRD), UMR 228 ESPACE DEV, 500, Rue Jean
11 François Breton 34093 Montpellier, France. danielle.mitja@ird.fr, eric.delaitre@ird.fr,
12 laurent.demagistri@ird.fr, therese.libourel@univ-montp2.fr

13 d. Institut de Recherche pour le Développement (IRD), 911 avenue Agropolis BP64501, 34394
14 Montpellier Cedex 05, France. michel.petit@ird.fr

15

16 *Corresponding author :

17

18 Alessio Moreira dos Santos : alessiomsag@gmail.com

19

20 **Abstract**

21 High spatial resolution images as well as image processing and object detection algorithms
22 are recent technologies that aid the study of biodiversity and commercial plantations of forest
23 species. This paper seeks to contribute knowledge regarding the use of these technologies by
24 studying randomly dispersed native palm tree. Here, we analyze the automatic detection of
25 large circular crown (LCC) palm tree using a high spatial resolution panchromatic GeoEye
26 image (0.50 m) taken on the area of a community of small agricultural farms in the Brazilian
27 Amazon. We also propose auxiliary methods to estimate the density of the LCC palm tree
28 *Attalea speciosa* (babassu) based on the detection results. We used the “Compt-palm”
29 algorithm based on the detection of palm tree shadows in open areas via mathematical
30 morphology techniques and the spatial information was validated using field methods (i.e.
31 structural census and georeferencing). The algorithm recognized individuals in life stages 5
32 and 6, and the extraction percentage, branching factor and quality percentage factors were
33 used to evaluate its performance. A principal components analysis showed that the structure
34 of the studied species differs from other species. Approximately 96% of the babassu
35 individuals in stage 6 were detected. These individuals had significantly smaller stipes than
36 the undetected ones. In turn, 60% of the stage 5 babassu individuals were detected, showing
37 significantly a different total height and a different number of leaves from the undetected
38 ones. Our calculations regarding resource availability indicate that 6,870 ha contained 25,015
39 adult babassu palm tree, with an annual potential productivity of 27.4 t of almond oil. The
40 detection of LCC palm tree and the implementation of auxiliary field methods to estimate
41 babassu density is an important first step to monitor this industry resource that is extremely
42 important to the Brazilian economy and thousands of families over a large scale.

43 **Keywords:** Shadow detection; Mathematical morphology; Density estimate; Remote sensing;
44 Brazilian Amazon

45

46 **1. Introduction**

47 The babassu (*Attalea speciosa* Mart. ex Spreng.) is a palm tree species native to dense
48 and humid forests that is distributed across approximately 200,000 km² of forests and
49 savannas in Brazil, with optimal development in secondary environments (Anderson and
50 Anderson, 1985; May et al., 1985; Barot et al., 2005; Santos and Mitja, 2011; Coelho et al.,
51 2012). Recent research emphasized the importance of this palm tree to industry, given its
52 potential for biodiesel production (Da Rós et al., 2014) and bioenergy (Protásio et al., 2014);
53 to ethnobotany, given its use diversity (Araujo and Lopes, 2012; Martins et al., 2014); to
54 anthropology, given its economic and social importance for small farmers (Porro and Porro,
55 2014); and to medicine because babassu palm trees can become infested with triatomines,
56 which transmit Chagas disease (Dias et al., 2014). Recently, babassu oleaginous almonds
57 were considered as the third most important non-wood product of plant extractivism in Brazil
58 (89,739 t/\$56.7 million in 2013; IBGE, 2013). Nevertheless, a gap exists between the
59 knowledge of this species and use of technologies that might aid in its management and
60 sustainable exploitation.

61 In forest plantations, information on tree or palm tree density is obtained using remote-
62 sensing techniques that aid in productivity monitoring, planning and management of African
63 oil palm tree (Shafri et al., 2011; Srestasathiern and Rakwatin, 2014) and eucalypt (Whiteside
64 et al., 2011; Zhou et al., 2013) plantations. The spatial information provided regarding the
65 number of trees or palm trees enables (among other things) the identification of excessive
66 mortality areas (Zhou et al., 2013) and the prediction of production dates (Malek et al., 2014),
67 which are essential for resource management and conservation (Engler et al., 2013).

68 As an alternative to time-demanding tasks of individually counting trees or palm trees
69 in the field, automatic-detection methods were developed using high spatial resolution
70 images. The primary objective of this detection is to determine the location of the tree or palm
71 tree crowns in an image (Srestasathien and Rakwatin, 2014). Studies apply different
72 techniques to delimit tree and palm tree crowns based on the value of each pixel in the image
73 (Erikson and Olofsson, 2005). Some of the techniques used include the marked-point process
74 (MPP) via Worldview 1 and Worldview 2 multispectral images (Zhou et al., 2013), the
75 maximum local detection method using Kodak DCS 460 CIR and UltracamD digital camera
76 images (Pouliot et al., 2002; Hirschmugl et al., 2007), and a technique based on the structure
77 of the elements using an airborne AISA hyperspectral image (Shafri et al., 2011). These
78 techniques are generally used for homogeneous forest plantations disposed along a line; not
79 having other species within the plantation avoids confusion when analyzing the images.

80 The mapping of tree crowns in non-planted areas (i.e., those dispersed in cultivated
81 areas or in homogeneous or heterogeneous natural forests) can be based on the detection of
82 crowns via object-oriented classification using IKONOS and GeoEye images (Aouragh et al.,
83 2013), the wavelet-transform technique (Zhang et al., 2006; Ghiyamat and Shafri, 2010), or
84 via supervised classification techniques such as spectral angle mapper, a linear discriminant
85 analysis, and the maximum likelihood method (Clark et al., 2005), both techniques use an
86 airborne HYDICE hyperspectral image.

87 Few studies have used image-based palm tree detection directed toward regular
88 African oil palm tree plantations. Currently, babassu plantations are not found in Brazil,
89 which might explain why this species has not yet been evaluated using automatic detection
90 via images from recent satellites such as GeoEye, Ikonos, Worldview or Quickbird (which
91 offer a spatial resolution of less than 1 m). The development of images with a resolution of
92 less than 1 m enabled the more precise detection of small objects such as tree crowns in

93 agricultural areas and their different shapes (Aouragh et al., 2013) using canopy delineation
94 algorithms (Culvenor, 2002).

95 Although the classic algorithms developed for crown delineation fundamentally
96 assume that the center of a crown appears radiometrically brighter than its edge (Culvenor,
97 2002), the algorithm developed by Demagistri et al. (2014), adapted for open environments,
98 extracts the image pixels that correspond to shadows using the mathematical morphology
99 technique (Serra, 1982; Haralick et al., 1987). This algorithm permits the detection of palm
100 trees in pastures and agricultural plantations with low-to-average palm tree density. This
101 image analysis technique is important (Soille and Pesaresi, 2002; Giada et al., 2003) for the
102 detection of individual trees (Jiang and Lin, 2013) and other objectives. This technique is
103 known as “morphology” because it analyses the content and shape of the object and called
104 “mathematical” because it is based on set theory, integral geometry, and algebraic structure
105 (Giada et al., 2003). Therefore, this algorithm has been used to detect the babassu palm tree in
106 open agricultural environments.

107 Studies on tree and palm tree-crown detection do not usually employ field methods to
108 validate the spatial information (Clark et al., 2005; Zhang et al., 2006; Hirschmugl et al.,
109 2007; Ghiyamat and Shari, 2010; Shafri et al., 2011; Aouragh et al., 2013; Malek et al., 2014;
110 Srestasathiern and Rakwatin, 2014). When used, these methods are typically restricted to
111 measure crown diameter and individual density (Pouliot et al., 2002, Zhou et al., 2013),
112 although other structural characteristics of the individuals might affect their detection using
113 the algorithm. Therefore, understanding these characteristics is an important step to improve
114 the reliability of spatial information.

115 A large diversity of palm trees exists in the Amazon region, including 195 species and
116 35 genera. The most important genera include *Attalea* and *Astrocaryum*, each with 28 species
117 (Pintaud et al., 2008). In addition to *Attalea speciosa* (babassu), other large circular crown

118 (LCC) species such as *Attalea maripa* (inajá), *Astrocaryum aculeatum* (tucumã), *Oenocarpus*
119 *bacaba* (bacaba) and *Mauricia flexuosa* (buriti) are distributed in an isolated and random
120 manner (D. Mitja, Personal communication). Because no methods are described in the
121 literature that enable differentiation among LCC palm tree types using a high-resolution
122 image, estimating the density of a species of interest (e.g., the babassu) using automatic
123 detection is a real challenge.

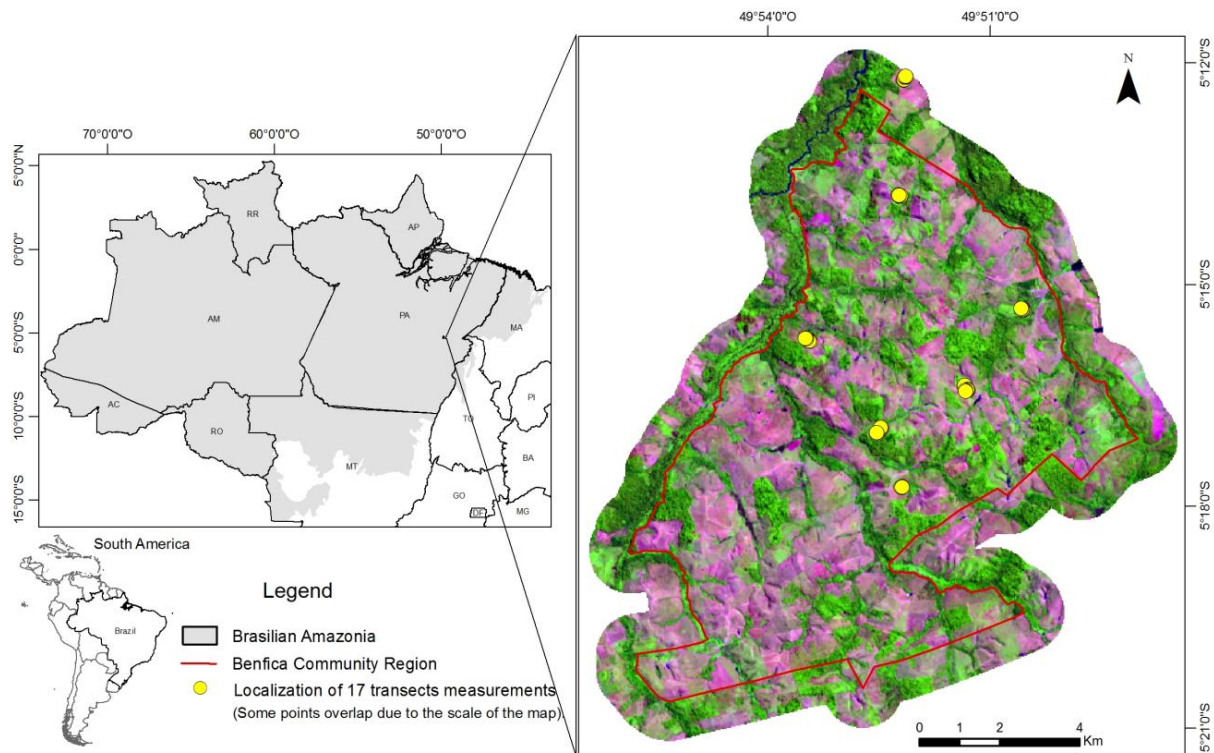
124 In the present study, we analyzed the automatic detection of LCC palm trees using a
125 high spatial resolution panchromatic image (GeoEye1 sensor, 0.50-m resolution, July/2013)
126 taken on a community of small farms in the Brazilian Amazon after validating the remote-
127 sensing data using photo-interpretation and field methods. Based on the automatic detection
128 results, we implemented auxiliary field methods to estimate babassu density.

129

130 **2. Material and Methods**

131 2.1. Characterization of the study area

132 This study was conducted in small farmlands in Benfica (S 05°16'20", W 49°50'25"),
133 (Itupiranga State of Pará (PA), southeast of the Brazilian Amazon) (Fig. 1). This site has
134 9,501 ha, and its occupation started in 1986 successively by farmers and settlers. Its land
135 regularization was consolidated by the National Institute of Colonization and Agrarian
136 Reform (Instituto Nacional de Colonização e Reforma Agrária; INCRA) in 1996 (Arnauld de
137 Sartre, 2004). The latest estimate indicated 183 agricultural establishments and approximately
138 1,000 people in the community (Ritter et al., 2009).



139

140 Fig. 1. The study area (Benfica, PA), located southeast of the Brazilian Amazon, shown by a
 141 Landsat 8-OLI 2013 image (RGB: B6, B5, B4).

142 *Two transects were near but outside the limit of Benfica community.

143

144 The vegetation in this area is upland tropical forest, characterized by the presence of
 145 lianas and palm trees (Mitja and Miranda, 2010). The dense forest has a canopy between 25
 146 and 30 m in height, although some trees (e.g., *Bertholletia excelsa* H.B.K) reach a height of
 147 over 50 m (Bertrand, 2009). Landsat 8-OLI images taken in 2013 (Fig. 1) showed that
 148 primary and old secondary forests (in dark green colors) covered 34% of the area in Benfica,
 149 whereas degraded pastures or pastures with little cover (in purple and pink colors) represented
 150 31%; pastures in good states and young secondary forests (in light green colors) accounted for
 151 31% of the area (Eric Delaître, Personal communication).

152 When forests are converted into pastures, some palm trees and timber species are
 153 maintained (Mitja et al., 2008; Santos and Mitja, 2011), thereby contributing to the

154 composition of the local landscape that includes pastures containing woody species (15%) and
155 pastures with babassu (12%; Sampaio, 2008). The high reproductive plasticity of babassu
156 favors its development in agricultural areas (Barot et al., 2005) because the use of fire for
157 agricultural management contributes to the germination and regeneration of babassu
158 individuals (Mitja and Ferraz, 2001). Thus, the different densities of the babassu in the study
159 area are partially a result of its resilience to natural and anthropogenic disturbances, insofar as
160 (similar to some other species) it has particular morphological characteristics and reproductive
161 strategies that influence its phenology and gene flow (Montúfar et al., 2011).

162 The climate is tropical humid with average temperature of 26°C. The average annual
163 rainfall is 1,700 mm, distributed irregularly throughout the year. The region's two seasons are
164 defined by the movements of the intertropical convergence zone: the rainy season, which
165 typically lasts approximately 8 months (October to May); and the dry season, which typically
166 lasts 4 months (June to September; Bertrand, 2009).

167 A variety of soils exists along the toposequences: (i) oxisol, with a thick B horizon
168 rich in ferruginous nodules; (ii) cambisol, with an incipient B horizon and a C horizon located
169 close to the surface; and (iii) gleysol, with an A horizon rich in organic matter, A and B
170 horizons with little clay, and hydromorphy along the entire profile (Ritter et al., 2009). As is
171 the norm for most arable lands in the Amazon, the soil fertility of the study area is low (Ritter
172 et al., 2009).

173

174 2.2. Field data

175 The information obtained in the field enabled the definition of the proportion of
176 babassu in the set of LCC palm trees. There are five LCC palm tree species in Benfica, three
177 are more frequent, babassu, inajá and tucumã, and two rare species, bacaba and buriti (Santos

178 and Mitja, 2011; Danielle Mitja, Personal communication). In a 487 ha pasture area of the
179 study site (=62-plots), we observed that 93.6% of the LCC palm trees found were babassu.
180 This result was used to estimate the babassu density based on the automatic LCC palm tree
181 detection results.

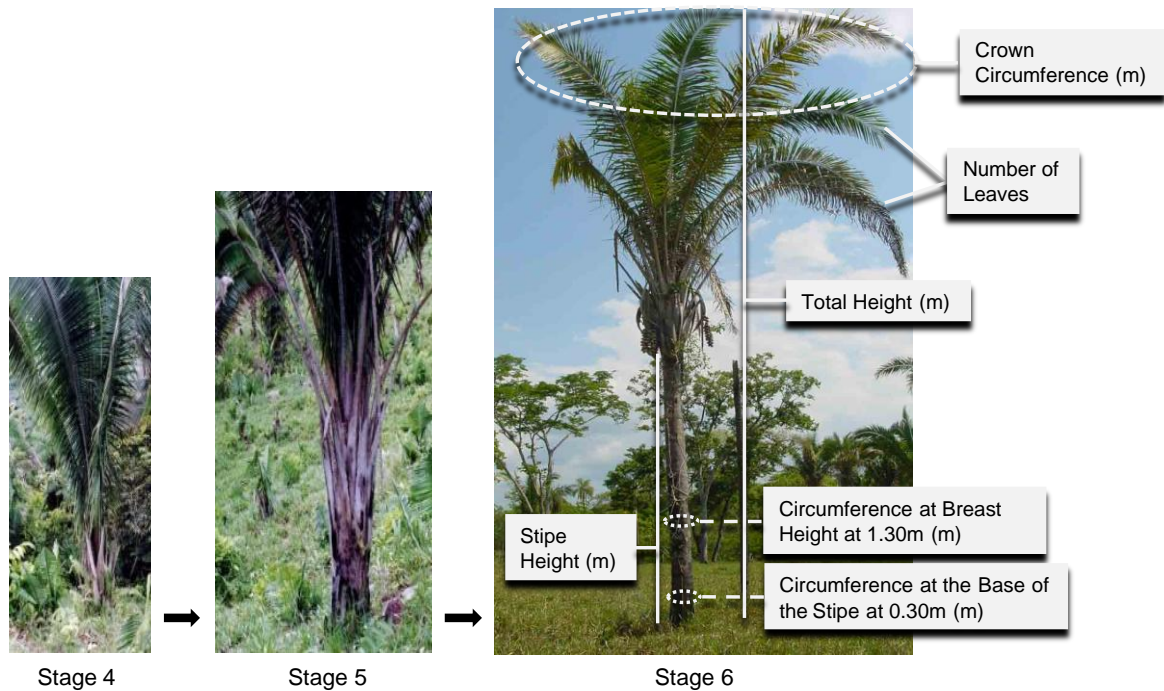
182 A total of 17 transects were sampled in pastures of different ages (1, 3, 5, 7 and 9
183 years), with a total sampling area of 1.3 ha (Fig. 1). In these transects, we noted that 46.51%
184 of the detected palm trees belonged to stage 5, whereas 53.49% belonged to stage 6.

185 A total of 150 babassu across three development stages were inventoried in the pasture
186 areas. Out of these babassu, 105 were in stage 6 (adults with an aerial stipe and signs of male
187 and/or female reproductive organs), 30 were in stage 5 (juvenile with an aerial stipe,
188 regardless of sheath coverage, and without the signs of male or female reproductive organs),
189 and 15 were in stage 4 (juvenile with a terminal bud at the soil surface level, with well-visible
190 leaf sheaths).

191 The structural information obtained in the field included circumference at breast
192 height, circumference at the base of the stipe, number of leaves, total height, stipe height, and
193 crown circumference (Fig. 2). This structural information was also obtained for two other
194 LCC palm trees species, inajá (31 individuals) and tucumã (30 individuals).

195 All these palm trees were georeferenced using the global positioning system (GPS;
196 model: GARMIN 62stc) to be located in the GeoEye 2013 image and identify the individuals
197 that had been detected using the detection algorithm.

198



199

200 Fig. 2. Life-cycle stages of the babassu palm trees studied in Benfica and the
 201 structural information obtained

202

203 2.3. Remote sensing image

204

205

206

207

208

209

210

211

212

213 2.4. LCC palm tree detection algorithm development and evaluation

214 An “Compt-palm” algorithm adapted to open environments was developed to detect
215 the following LCC palm trees: babassu, inajá, tucumã, bacaba and buriti (Demagistri et al.,
216 2014). A panchromatic GeoEye 2009 image of Benfica was used in the algorithm-
217 development process. At first, shadows palm trees are extracted using mathematical
218 morphology techniques; then each shadow object (which corresponds to a potential palm tree)
219 undergoes a supervised classification by calculating a decision coefficient used to assign that
220 object a particular class label between “palm tree shadow” and “other shadow”.

221 The shadow extraction protocol proceeds as follows:

- 222 i) Smoothing of the panchromatic image: this first filter removes the noise from the
223 image;
- 224 ii) Local adaptive filtering based on the mean and standard deviation of a moving
225 window: zones with a strong local contrast (i.e. the shadows) are extracted;
- 226 iii) Morphological closing: the first step in cleaning the shadow extraction results;
- 227 iv) Connected components extraction: labeling of independent shadow objects;
- 228 v) Object size thresholding: the second step in cleaning the shadow extraction results.

229 Afterwards, shadow objects are classified using a supervised classification based on a
230 distance criterion and a decision rule process. These steps are detailed below:

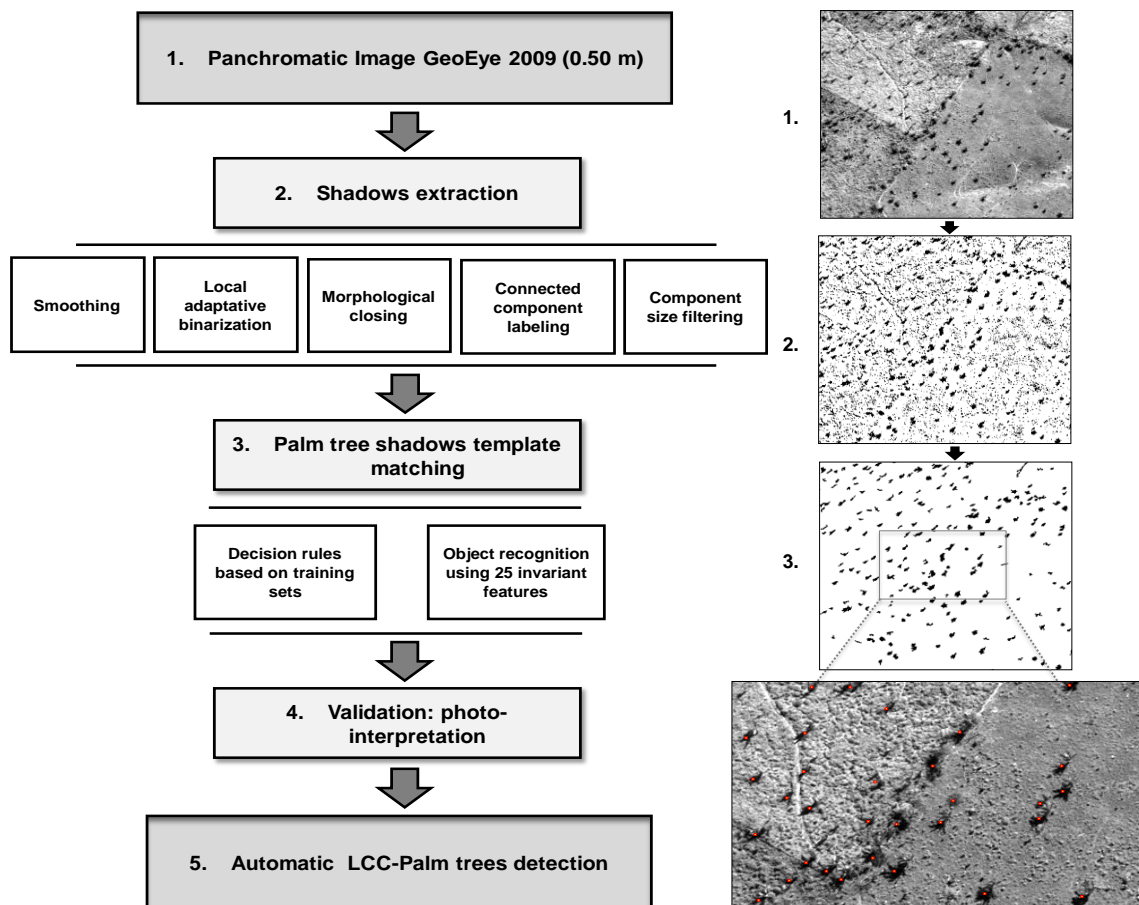
- 231 i) Classifier training with two sets of shadow images: 75 cropped images of “palm
232 tree shadows” and 75 cropped images of “other shadows”; 25 normalized shape
233 characteristics and invariants are computed on the whole set of the cropped images
234 (see below for some details).
- 235 ii) Calculation of classifier entry parameters for each potential palm tree shadow and
236 selection of the 5 closest shadow objects (Euclidian distance computation) within
237 the training set.

238 iii) Score calculation, according to the class of the closest shadow objects, enabling
239 appropriate classification of each shadow.

240 To characterize the palm tree shadows, we worked with the shape characteristics and
241 invariant described in Torres-Méndez et al. (2000). For each shadow image, we first compute
242 its moment of inertia (1 parameter). Then, using 12 concentric circles centered on the shadow
243 centroid we count for each circle the number of intensity changes that occur (shadow/no-
244 shadow) and the normalized difference of the two largest arcs that are not part of the shadows
245 (12x2 parameters).

246 The result is a list of points in image or cartographic coordinates that can be compared
247 with data obtained using image photo-interpretation. The steps by which the LCC palm tree
248 detection algorithm proceeds are shown in Fig. 3.

249



250

251 Fig. 3. Representation of the steps of the LCC palm trees automatic detection
252 algorithm (adapted from Demagistri et al., 2014)

253

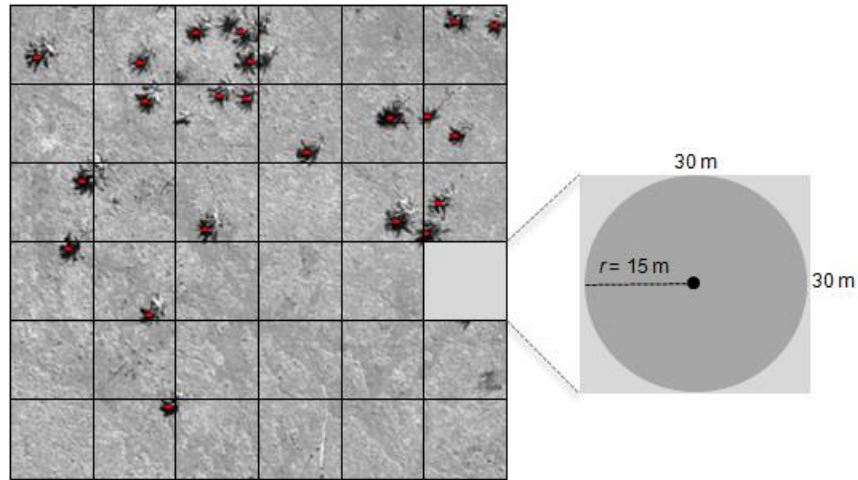
254 The algorithm was validated using image photo interpretation via a sample of 334
255 points observed over 16 cells of 1-ha, distributed in pastures of low and average babassu
256 density in the study area.

257 To evaluate the precision and quality of the algorithm used, were considered the
258 factors adopted by Shufelt (1999) and Luo et al. (2014); these factors can be based on image
259 pixel classifications or on object shape and consider the numbers of true positives (TP), false
260 positives (FP), and false negatives (FN). The first factor is the extraction percentage, given by
261 the expression $100*TP/(TP+FN)$, which can be understood as a measure of shadow extraction
262 performance. The second factor is the branching factor, given by FP/TP , which measures
263 delineation performance. The third factor is the quality percentage, given by
264 $100*TP/(TP+FP+FN)$, a general measure of method performance. According to Shufelt
265 (1999), the use of these three measures completely evaluates model performance.

266

267 2.5. Density map and calculation of the babassu resource estimate

268 The palm tree location map produced by applying the algorithm to open environments
269 on the GeoEye-1 2013 image was processed using ArcGis 10.2.2 with the Point Density tool
270 to obtain the palm tree density map. The parameters used were the size of the raster cells (30-
271 m) and the size and shape of the point search neighborhood (a 15 m radius circle, Fig. 4). The
272 number of individuals per ha was used to calculate palm density.



273

274 Fig. 4. Representation of the parameters used to elaborate the density map

275

276 The number of LCC palms actually present (B) was defined as:

277 $B=A-(A \times FP)/100+(A \times FN)/100$; where: A = number of points indicated by the

278 algorithm as corresponding to LCC palm trees; FP = False Positive; FN = False Negative.

279 Then, based on information from Santos and Mitja (2011) was calculated the number of

280 babassu as 93.6% of the total number of palm trees.

281 Therefore, we can calculate the number of babassu palm trees (C) from the total LCC

282 palm trees (B).

283
$$C=(B \times 93.6)/100$$

284 To obtain the proportion of stage 5 and 6 individuals in the pastures we use a total

285 density of palm trees in of 17 transects, with 46.51% of stage 5 and 53.49% of stage 6.

286 Therefore, we calculated the total numbers of babassu palm trees (detected and undetected) in

287 stage 5 (V) and stage 6 (W) present in open areas in Benfica.

288 Adult palm trees (stage 6):

289
$$\left\{ \begin{array}{l} C=V+W \\ \text{With } V=(46.51\% \text{ of } C), \text{ and} \\ W=(53.49\% \text{ of } C) \end{array} \right.$$

290

291

292 Finally, despite the high variation in the amount of oil extracted according to the used
293 method, we estimated the annual potential productivity of almond oil of Benfica, using (i) the
294 estimated density of adults at Benfica and (ii) literature data on fruit production (24 kg of
295 fruits / palm / year on average - Anderson, 1983), seed production (1 kg of seeds from 13 kg
296 of fruits – Gonsalves, 1955), and oil production (1 kg of crude oil from 1.68 kg of almonds -
297 Frazão, 2001).

298

299 2.6. Statistical analyses

300 A principal components analysis (PCA) was used to verify differences in the structural
301 characteristics of LCC palm trees species. The significance of the PCA was determined using
302 the Monte Carlo permutation test at $p < 0.05$.

303 The structural characteristics of babassu palm trees at stages 5 and 6 were compared
304 using the non-parametric Wilcoxon test, as were the structural characteristics of the
305 individuals at each stage based on whether they were detected or not, using the algorithm. All
306 statistical analyses were performed using the software R 3.1.2 (R Core Team, 2014) with the
307 packages ADE-4 (Dray and Dufour, 2007; Dray et al., 2007).

308

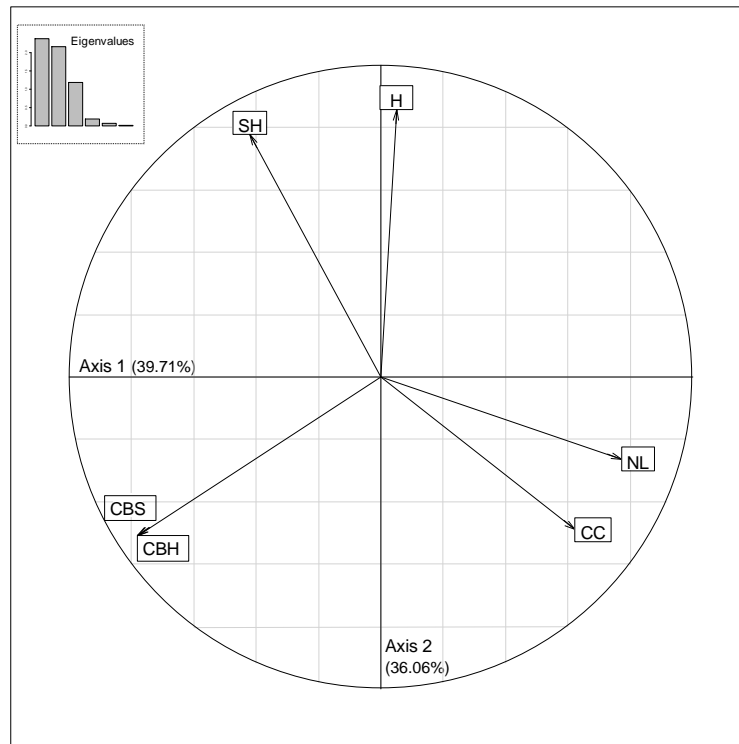
309 **3. Results**

310 3.1. Structural characteristics of the LCC palm trees

311 The use of the shadow-detection algorithm detected the babassu palm trees and also
312 other palm tree, especially those dominant in Benfica, such as inajá and tucumã.

313 In contrast, the PCA of the structures of the babassu, inajá and tucumã palm trees (all
314 belonging to stage 6, i.e., adults) showed that the LCC palm trees differed structurally. The
315 first two PCA axes explained 75.77% of the variance in the scatterplot. Axis 1 explained

316 39.71% of the variance, and the structural variables that contributed the most to this axis were
317 circumference at breast height, circumference at the base of the stipe, number of leaves. The
318 second axis explained 36.06% of the variance, and its most important variables were total
319 height, stipe height (Fig. 5).



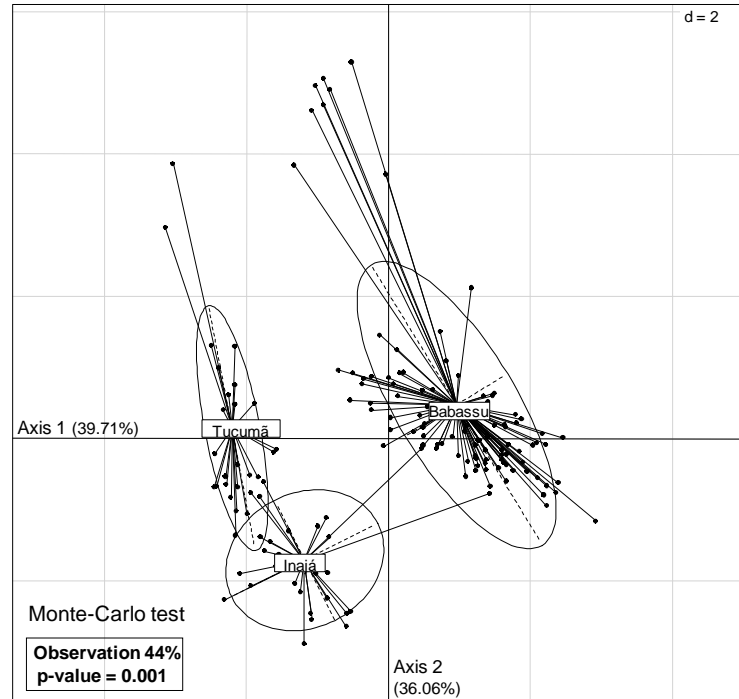
320

321 Fig. 5. The PCA using the structural variables of three palm tree species in Benfica.
322 Circumference at breast height (CBH), circumference at the base of the stipe (CBS),
323 number of leaves (NL), total height (H), stipe height (SH), and crown circumference (CC).

324

325 In the PCA formed by the first and second axes, the structural variables were grouped
326 according to palm tree type: babassu, injá, and tucumã. According to a Monte Carlo test with
327 999 permutations, 44% of the data variance was explained by palm tree species, and this value
328 was significant ($p=0.001$; Fig. 6).

329



330

331 Fig. 6. The first and second axes of the PCA regarding the structural variables of the species
 332 *Attalea speciosa* (Babassu), *Attalea maripa* (Inajá) and *Astrocaryum aculeatum* (Tucumã) in
 333 Benfica.

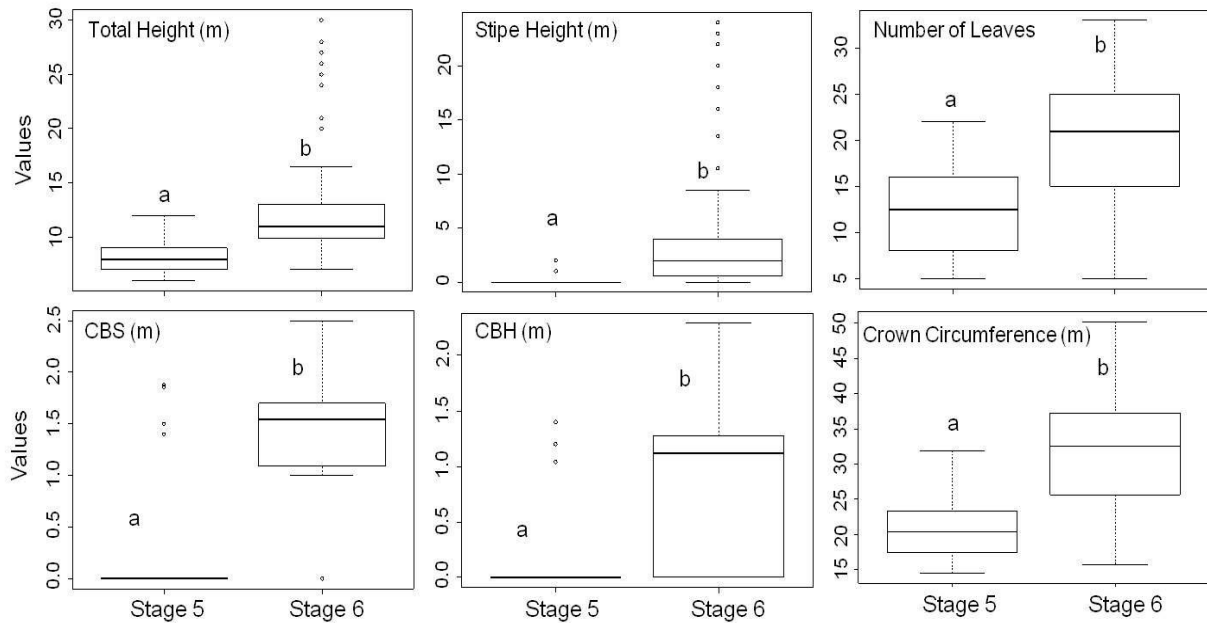
334

335 3.2. The structural characteristics of the individuals detected/undetected by the algorithm

336 The algorithm did not detect any of the stage 4 babassu palm trees identified in the
 337 field.

338 When comparing the morphological characteristics of the stage 5 and 6 palm trees
 339 using a boxplot (Fig. 7), we observed that the stage 6 palm trees had higher values and
 340 significantly differed from those in stage 5 (Wilcoxon test, $p < 0.0001$) for all the structural
 341 characteristics analyzed.

342



343

344 Fig. 7. A comparison of the morphological characteristics of stage 5 (n=30) and stage 6
 345 (n=105) *Attalea speciosa* palm trees. Each box of the plot extends from the data of quartiles 1
 346 and 3; the horizontal lines within each box represent the median; and the circles at the
 347 extremities represent the values close to the box. The different letters indicate that the means
 348 are significantly different (Wilcoxon test, $p < 0.0001$). CBH, circumference at breast height;
 349 CBS, circumference at the base of the Stipe.

350

351 Approximately 96% of the stage 6 palm trees identified in the field were detected
 352 using the algorithm based on their shadows; only 4% remained undetected. The comparison
 353 between the mean structural characteristics of the detected and undetected individuals
 354 revealed a significant difference (Wilcoxon test, $p < 0.05$) only for the mean stipe height,
 355 which was greater for detected palm trees than undetected palm trees (Table 1).

356

357 Approximately 60% of the stage 5 babassu palm trees identified in the field were
 358 detected using the algorithm, and 40% were not detected (Table 1). The total height and the
 number of leaves values of the detected and undetected individuals significantly differed

359 (Wilcoxon test, $p < 0.05$), with detected individuals having larger morphological characteristic
 360 values than their undetected counterparts.

361

362 Table 1. The morphological characteristics of stage 5 and 6 babassu palm trees, regardless of
 363 detection using the algorithm in open areas. The means were compared using the non-
 364 parametric Wilcoxon test. Ns: not significant; *: $p < 0.05$

Stage 5 (n=30)	% Individuals	Total Height (m)	Stipe Height (m)	Number of Leaves	Circumference at the Base of the Stipe (m)	Circumference at Breast Height (m)	Crown Circumference (m)
Undetected	40	7.33	0.00	9.33	0.00	0.00	20.37
Detected	60	8.25	0.38	14.61	1.66	1.21	21.32
		*	Ns	*	Ns	Ns	Ns

Stage 6 (n=105)	% Individuals	Total Height (m)	Stipe Height (m)	Number of Leaves	Circumference at the Base of the Stipe (m)	Circumference at Breast Height (m)	Crown Circumference (m)
Undetected	4	11.25	0.50	15.75	1.68	1.54	28.63
Detected	96	12.38	3.94	19.76	1.60	1.26	31.87
		Ns	*	Ns	Ns	Ns	Ns

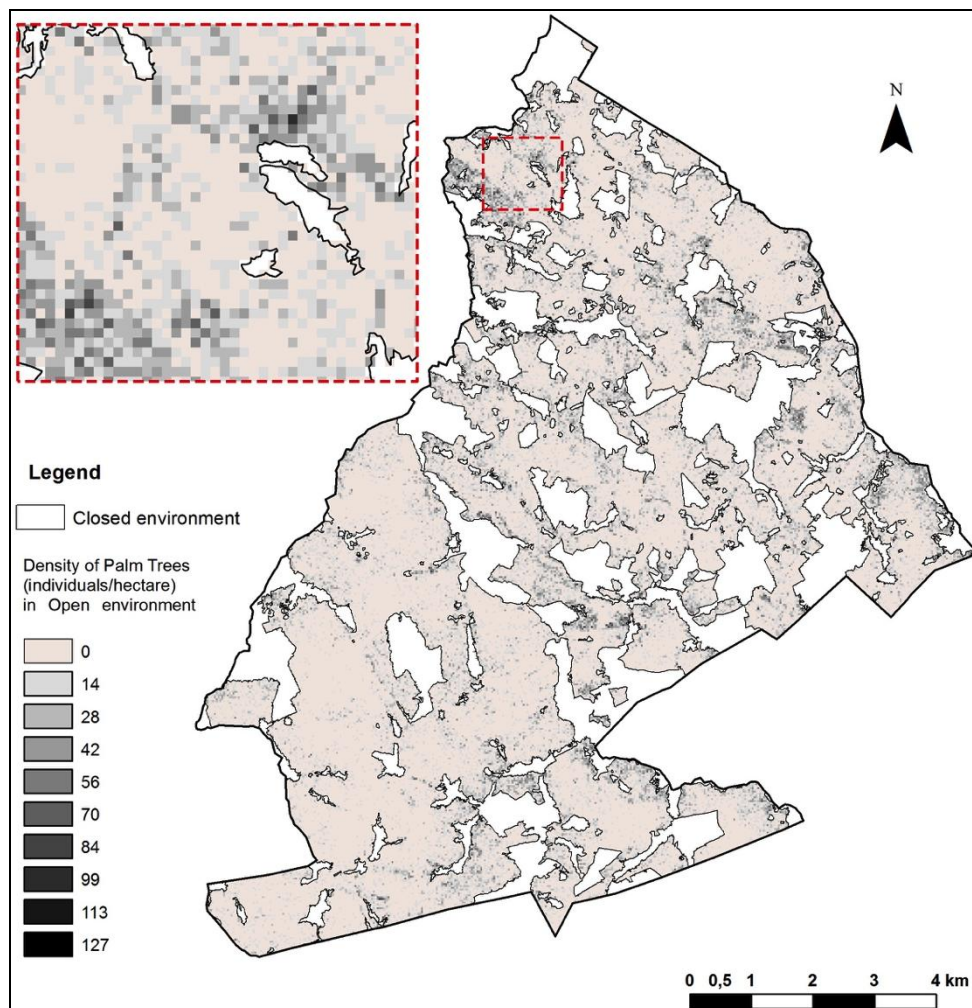
365

366

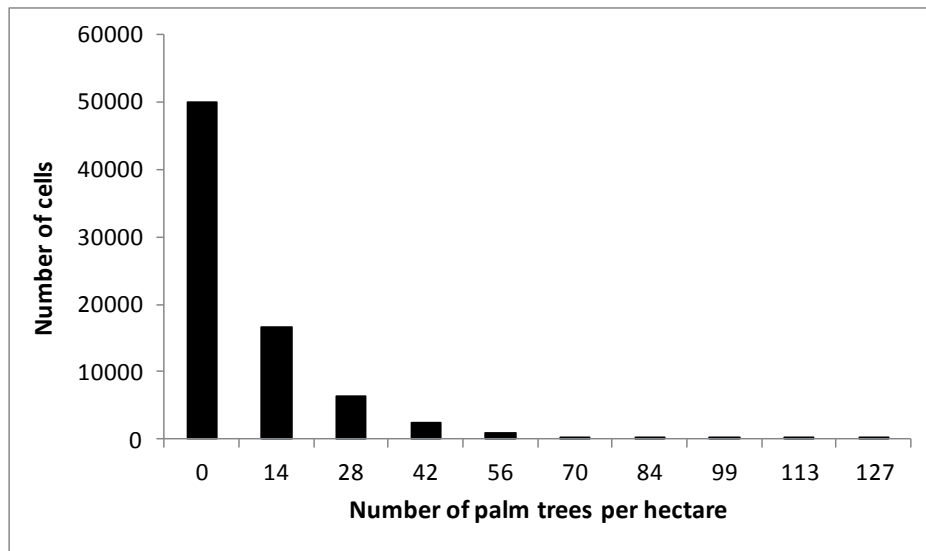
367 3.2. Algorithm quality and LCC palm tree density

368 When evaluating the performance of the algorithm used to automatically detect the
 369 LCC palm trees, we considered 334 points, in which 252 (75.45%) had been correctly
 370 identified by the algorithm (true positives), 55 (16.47%) points indicated by the algorithm that
 371 did not correspond to palm trees (false positives), and 27 (8.08%) points corresponding to
 372 palm trees that were not identified by the algorithm (false negatives). This analysis resulted in
 373 90.32% of Extraction, 0.218 of Branching factor, and 75.45% of Quality.

374 A palm tree density map (Fig. 8) was created after applying the open area algorithm to
375 the GeoEye1 2013 image. A total of 54,540 palm trees were detected in open vegetation in
376 Benfica communities (6,870 ha). In the study area, 65% of the cells had a null density, less
377 than 35% of the cells had a low LCC palm tree density (1 to 3 palm trees in a circle with a 15
378 m-radius, corresponding to 14 to 42 palm trees per ha), and less than 2% of the cells had an
379 average LCC palm tree density (4 to 9 palm trees in a circle with a 15 m-radius,
380 corresponding to 56 to 127 palm trees per ha) (Fig. 9). The average-density areas were
381 localized and dispersed, whereas the low-density and null-density areas occupied a large
382 surface characterized by continuous areas.



383
384 Fig. 8. The LCC palm tree density map in Benfica based on the application of automatic
385 detection using the open areas algorithm with regard to the GeoEye1 2013 image



386

387 Fig. 9. A histogram of the number of cells as a function of palm tree density per ha in the
 388 density map obtained from the GeoEye1 2013 image

389

390 3.3. Babassu resource density productivity estimate

391 The 54,540 LCC palm tree points detected using the GeoEye1 2013 image of Benfica
 392 were corrected with regard to the algorithm's errors, resulting in 49,964 LCC palm trees
 393 actually present. By applying the 93.6% rate, we obtained 46,766 babassu palm tree based on
 394 the total number of LCC palm trees. Based on the field data of the proportion of stage 5
 395 (46.51%) and 6 (53.49%) palm trees in the study areas, we calculated 25,015 of babassu
 396 individuals in stage 6 (adults). Finally, we estimated that the adults in the open areas of
 397 Benfica have an annual potential productivity of 27.4 t of almond oil.

398

399 Discussion

400

401 4.1. The contribution of the field methods to validate the remote-sensing data

402 The local densities obtained via automatic detection are accurate; however, this
 403 information becomes much more efficient when combined with the data obtained via field

404 measurements (Zhou et al., 2013). In the present study, the measurements of the
405 morphological characteristics of palm trees and their cartographic coordinates were essential
406 to validate the remote-sensing data obtained using automatic detection.

407 As expected, it was not possible to differentiate between the LCC palm tree species in
408 images with a resolution of 0.50 m. However, these species have different structures. As Kahn
409 (1986) reported, the genera *Astrocaryum* and *Attalea* have a variety of forms: the species
410 *Astrocaryum aculeatum* has well-developed stipes (15 to 20 cm in diameter and 15 to 25 m in
411 height), and its leaflets are always placed on different planes (Kahn, 1986). Conversely,
412 *Attalea speciosa* has leaflets along the same plane (Kahn, 1986). *Attalea speciosa* can reach a
413 height of 10 to 30 m and have a stipe diameter of 30 to 60 cm (May et al., 1985; Lorenzi et
414 al., 2010), whereas *Attalea maripa* can reach a height of 7 to 24 m, have a stipe diameter of 20
415 to 40 cm, and leaves that are disposed in five directions (Lorenzi et al., 2010).

416 All of these forest palm trees grow in pastures and secondary vegetation (May et al.,
417 1985; Anderson and Anderson, 1985; Kahn, 1986) where they usually reach sexual maturity
418 earlier and grow to a smaller height than their counterparts in forests (Kahn, 1986). As palm
419 trees increase in height, their crowns become relatively narrower (Rich et al., 1986).

420 The PCA of the structure of the LCC palm trees (*Attalea speciosa*, *Attalea maripa* and
421 *Astrocaryum aculeatum*) present in the study area reinforces the differences in the architecture
422 among the species and suggests that stipe circumference (axis 1) and height (axis 2) are the
423 most important variables. Wang and Augspurger (2006) investigated the influence of palm
424 tree crown architecture on seedling recruitment on Barro Colorado Island in Panama and La
425 Selva forest in Costa Rica; based on a PCA, they concluded that the four palm tree species
426 studied at each site had different growth forms and crown architectures, with the number of
427 leaves and leaf area having the greatest influence on one axis and crown area influencing the
428 other two axes.

429 All of the structural variables analyzed in the present study influenced the shape of the
430 shadow of each species because different architectures can have more or less impact on the
431 way light propagates through vegetation (Wang and Augspurger, 2006). Because we used a
432 shadow-detection algorithm that also considers the shape of the shadow, differentiating
433 among LCC palm tree species might be possible if an image with a better spatial resolution
434 (i.e., less than 0.50 m) is used, given that these species have different structures. Moreover, it
435 might be possible to create a density map specific for the babassu palm tree (*Attalea speciosa*)
436 by extracting only the shadows that correspond to this species.

437 The validation of the information concerning stage 4, 5, and 6 of babassu palm tree,
438 with the aid of field methods (i.e., structural census and georeferencing) regardless of the
439 detection algorithm, enabled us to report which structural characteristics have a stronger
440 influence on their detection using a high spatial resolution image.

441 Almost all (96%) of the stage 6 babassu palm tree were detected using the high spatial
442 resolution satellite images, and only 4% did not have visible shadows and were not
443 automatically detected. The numbers of leaves and the crown widths of these individuals did
444 not significantly differ from those detected; however, their stipes were significantly smaller.

445 In turn, the stage 5 babassu palm tree were partially detected (60%). The 40% that
446 were not detected were shorter and had fewer leaves than those detected. However, it is
447 difficult to individually characterize the undetectable palm trees that belong to this stage
448 based on their morphological characteristics, as was done for stage 6. Some individuals with
449 similar morphological characteristics might not be detected because unmeasured factors might
450 also influence shadow formation. These factors might include i) the orientation of the palm
451 trees in relation to the sun when the image was captured by the sensor, ii) the leaf area (i.e.,
452 leaf width by blade length) of each individual (Wang and Augspurger, 2006), and iii) the
453 average distance between leaflets (Wang and Augspurger, 2006).

454 The algorithm most likely failed to detect stage 4 babassu palm trees because of the
455 spatial resolution of the image used (0.50 m), given that the shadow of these individuals is
456 nearly imperceptible or nonexistent under this resolution.

457 The babassu palm trees were divided into developmental stages to monitor the plant
458 growth over time across different environments (i.e., forests, pastures, and secondary forests).
459 Although this organization is biologically artificial, a continuum in babassu growth exists
460 from the seedling to adult stages. The significant difference in the structure of individuals
461 between stages 5 and 6 indicates that the separation of individuals into these life stages was
462 well established. Although certain stage 5 individuals were similar to those in stage 6, stage 6
463 palm tree usually have higher morphological characteristic values that explain their
464 predominance among the detected plants. Because this species is native, non-cultivated, and
465 non-domesticated where no selection is yet practiced, significant between-plant variability
466 exists in the babassu population (Danielle Mitja, Personal communication).

467

468 4.2. Algorithm performance for the automatic detection of LCC palm trees

469 The result of the detection via the algorithm (75.45% quality) was promising given
470 that it was applied to natural, non-planted areas. In commercial plantations of the African oil
471 palm tree, organized along lines and without other species besides the cultivated one, the
472 detection precision reaches 90% (Srestasathiern and Rakwatin, 2014); when high spatial
473 resolution satellite images are used, this rate is approximately 95% (Shafri et al., 2011). Even
474 in homogeneous commercial plantations, however, issues might exist with the methods used
475 because of the presence of objects other than the cultivated species, which are often detected
476 as false positives (Srestasathiern and Rakwatin, 2014). Future studies should use texture
477 information to suppress the presence of objects other than the species of interest
478 (Srestasathiern and Rakwatin, 2014).

479 In the present study, 75.45% of the LCC palm trees were successfully detected.
480 However, this rate might be improved by decreasing the number of false positives (as reported
481 above) and that of false negatives (for groups composed of 2 or 3 palm trees, only 1 palm tree
482 is detected). In the case of a false negatives, the palm tree crowns might overlap, resulting in a
483 single shape that differs from that of an isolated palm tree. Zhou et al. (2013) also faced the
484 challenge of crown overlap; these authors were unable to detect the canopies of closely
485 spaced trees on a Eucalyptus plantation. Moreover, Shari et al. (2011) noted that the crown-
486 detection method applied worked well only for isolated African oil palm trees. All these
487 studies used a spatial resolution of 0.50 m or greater. Better resolutions (0.10 – 0.30 m) for
488 example using drones, and the improvement of the algorithm should decrease this error.

489 Using the LCC palm tree density map, we observed that this algorithm might be used
490 to estimate the occurrence of palm trees present in the open area of interest using a high
491 spatial resolution image (0.50 m). One of the major advantages of mapping species of interest
492 via high-resolution images compared with forest censuses is that this information can be
493 obtained for large areas (Zhou et al., 2013), as it is the case in the present study, especially
494 because multispectral and hyperspectral images are becoming more accessible.

495

496 4.3. The potential use of this technique for babassu productivity monitoring, planning, and
497 management

498 Automatic mapping in commercial plantations seeks to identify high-mortality points
499 (Zhou et al., 2013) and the plants affected by disease (Shari et al., 2011; Johansen et al., 2014)
500 to define management practices. In turn, the density map of the LCC palm trees over large
501 areas proposed here, provides a wide view of resource distribution along the entire basin and
502 enables the identification of areas with greater densities, access and productive potential,
503 favoring the planning of resource exploitation and management based on the interests of land

504 owners or producer associations. In addition, given the risk of overexploitation and species
505 extinction, environmental agencies might use this tool to aid in the inspection of areas where
506 babassu felling is prohibited by law (Porro et al., 2011) or to monitor the variation in resource
507 density over time, as suggested by Aouragh et al. (2013) and Zhou et al. (2013) with regard to
508 tree species.

509 Remote sensing, very high spatial resolution images, image processing, and object
510 detection algorithms have become some of the major technologies in geospatial research,
511 exploitation and monitoring of biodiversity (Bai et al., 2005; Clark et al., 2005; Schmidtlein et
512 al., 2012; Engler et al., 2013; Garrity et al., 2013; Lin, 2013; Laurin et al., 2014), and
513 commercial plantations of forest species of interest (Zhou et al., 2013; Srestasathiern and
514 Rakwatin, 2014). The present paper seeks to contribute to the use of this technology by
515 studying the native palm trees naturally and randomly dispersed and mixed with numerous
516 other species.

517 Because babassu is a native species that is adapted to secondary environments (May et
518 al., 1985; Anderson and Anderson, 1985), the expansion of the areas occupied by this species
519 is directly related to the advancement of the agricultural frontier in the Amazon through
520 deforestation (Teixeira, 2003). For many decades, this species has been the primary source of
521 income for farmers in North and Northeast Brazil (Teixeira, 2003; Porro et al., 2011; Porro
522 and Porro, 2014). However, the major hindrances within the production chain of babassu oil
523 in Brazil are the lack of a regular supply system for quality raw materials and the scarcity of
524 strategic partnerships with small farmers (Teixeira, 2003). The methods proposed in this study
525 regarding the density and production capacity estimates based on the results of automatic
526 detection will provide more precise results that might be used to simulate numerous
527 exploitation scenarios based on different systems of fruit harvest, adult density management

528 and species regeneration time. These systems might provide farmers with better plans of
529 action for the constant and sustainable use of the production potential of this palm tree.

530

531 **5. Conclusions**

532 The result of the automatic detection using the algorithm on a very high spatial
533 resolution image (75.45% quality) was promising, given that it was applied to natural, non-
534 planted areas.

535 The validation of the information concerning stage 4, 5, and 6 *Attalea speciosa*
536 (babassu) palm trees using field methods (i.e., structural census and georeferencing),
537 regardless of algorithm detection, provided information regarding which structural
538 characteristics have a greater influence on their detection in a very high spatial resolution
539 image. This step is important in the study of automatic detection using remote sensing images
540 of palm trees.

541 By itself, the use of the algorithm on very high spatial resolution images does not yet
542 deliver researchers a density map exclusively for babassu for farmers, associations or public
543 policies. However, the detection of LCC palm trees and the implementation of auxiliary field
544 methods to estimate the density of the species of interest is an important first step toward the
545 large-scale monitoring of this important resource, not only by the Brazilian industry and
546 economy but also by the thousands of families who depend on babassu extraction for
547 subsistence.

548

549 **Acknowledgments**

550 The authors thank the Institut de Recherche pour le Développement, whose support enabled
551 the development of this study. This project was also funded within the RELAIS
552 (CNPq/IRD/UFRJ) and CNES TOSCA/Babaçu projects. Thanks go to the farmers for their

553 receptivity and to Mr. Deurival da Costa Carvalho for his dedication to the fieldwork. This
554 study was performed with support from the Brazilian National Council for Scientific and
555 Technological Development (with a PhD scholarship sandwich in French) and the Brazilian
556 Federal Agency for the Support and Evaluation of Graduate Education (with a PhD
557 scholarship in Brazil).

558

559 **References**

560 Anderson, A.B., 1983. The biology of *Orbignya martiana* (Palmae), a tropical dry forest
561 dominant in Brazil. Thesis (PhD), University of Florida. 196 p.

562 Anderson, A.B., Anderson, S., 1985. A 'tree of life' grows in Brazil. *Nat. Hist.* 94 (12), 40-47.

563 Aouragh, M., Lacaze, B., Hotyat, M., Ragala, R., Aboudi, A.E., 2013. Cartographie et suivi
564 de la densité des arbres de l'Arganeraie (Sud-ouest du Maroc) à partir d'images de
565 télédétection a haute resolution spatiale. *Revue Française de Photogrammétrie et de*
566 *Télédétection* 203, 3-9.

567 Araujo, F.R., Lopes, M.A., 2012. Diversity of use and local knowledge of palm trees
568 (Arecaceae) in eastern Amazonia. *Biodivers Conserv* 21, 487–501. DOI:
569 10.1007/s10531-011-0195-9

570 Arnauld de Sartre, X., 2004. A Ruralisation of an Amazonian Frontier? In: *SLAS Annual*
571 *conference*. Society for Latin American Studies, 19 p.

572 Bai, Y., Walsworth, N., Roddan, B., Hill, D.A., Broersma, K., Thompson, D., 2005.
573 Quantifying tree cover in the forest–grassland ecotone of British Columbia using crown
574 delineation and pattern detection. *Forest Ecol Manag* 212, 92-100.
575 <http://dx.doi.org/10.1016/j.foreco.2005.03.005>

576 Barot, S., Mitja, D., Miranda, I., Meija, G.D., Grimaldi, M., 2005. Reproductive plasticity in
577 an Amazonian palm. *Evol Ecol Res* 7, 1051–1065.

578 Bertrand, G., 2009. Characterization of adaptive responses to water stress in the Southeast
579 Amazon in three forage species grown in monoculture and in association: *Brachiaria*
580 *brizantha*, *Leucaena leucocephala* et *Arachis pintoi*. Thesis (PhD), University of Paris-
581 Est. 181 p.

582 Clark, M.L., Roberts, D.A., Clark, D.B., 2005. Hyperspectral discrimination of tropical rain
583 forest tree species at leaf to crown scales. *Remote Sens Environ* 96, 375-398.

584 Coelho, R.F.R., Miranda, I.S., Mitja, D., 2012. Description of sucessional process at Benfica
585 Settlement Project, Southeastern of State of Pará, Eastern Amazon. *Bol Mus Para Emílio*
586 *Goeldi, Cienc Nat* 7(3), 251-282.

587 Culvenor, D.S., 2002. TIDA: An Algorithm for the Delineation of Tree Crowns in High
588 Spatial Resolution Remotely Sensed Imagery. *Computer & Geosciences* 28, 33-44.
589 [http://dx.doi.org/10.1016/S0098-3004\(00\)00110-2](http://dx.doi.org/10.1016/S0098-3004(00)00110-2)

590 Da Rós, P.C.M., Silva, W.C., Grabauskas, D., Perez, V.H., Castro, H.F., 2014. Biodiesel from
591 babassu oil: Characterization of the product obtained by enzymatic route accelerated by
592 microwave irradiation. *Ind Crop Prod* 52, 313-320.
593 <http://dx.doi.org/10.1016/j.indcrop.2013.11.013>

594 Demagistri, L., Mitja, D., Delaitre, E., Shahbazkia, H., Petit, M., 2014. Palm trees detection
595 with very high resolution images, comparison between Geoeye and Pléiades sensors.
596 <http://www.pleiades2014.com/presentations-2014> (accessed 14.01.17).

597 Dias, F. B., Quartier, M., Diotaiuti, L., Mejía, G., Harry, M., Lima, A. C., Davidson, R.,
598 Mertens, F., Lucotte, M., Romaña, C.A., 2014. Ecology of *Rhodnius robustus* Larrousse,
599 1927 (Hemiptera, Reduviidae, Triatominae) in *Attalea* palm trees of the Tapajós River
600 Region (Pará State, Brazilian Amazon). *Parasit Vectors*. 7, 154.

601 Dray, S., Dufour, A.B., 2007. The ade4 package: implementing the duality diagram for
602 ecologists. *Journal of Statistical Software* 22(4), 1-20.

603 Dray, S., Dufour, A.B., Chessel, D., 2007. The ade4 package-II: Two-table and K-table
604 methods. *R News* 7(2), 47-52.

605 Engler, R., Waser, L.T., Zimmermann, E., Schaub, M., Berdos, S., Ginzler, C., Psomas, A.,
606 2013. Combining ensemble modeling and remote sensing for mapping individual tree
607 species at high spatial resolution. *Forest Ecol Manag* 310, 64-73.

608 Erikson, M., Olofsson, K., 2005. Comparison of three individual tree crown detection
609 methods. *Mach Vision Appl* 16(4), 258-265.

610 Frazão, J.M.F., 2001. Alternativas econômicas para agricultura familiar assentadas em áreas
611 de ecossistemas de babaquais. Relatório Técnico, Governo do Estado do Maranhão, São
612 Luis. 120pp.

613 Garrity, S.R., Allen, C.D., Brumby, S.P., Gangodagamage, C., McDowell, N.G., Cai, D.M.,
614 2013. Quantifying tree mortality in a mixed species woodland using multitemporal high
615 spatial resolution satellite imagery. *Remote Sens Environ* 129, 54-65.
616 <http://dx.doi.org/10.1016/j.rse.2012.10.029>

617 Ghiyammat, A., Shafri, H.Z.M., 2010. A review on hyperspectral remote sensing for
618 homogeneous and heterogeneous forest biodiversity assessment. *Int J Remote Sens* 31(7),
619 1837-1856.

620 Giada, S., Groeve, T.D., Ehrlich, D., Soille, P., 2003. Information extraction from very high
621 resolution satellite imagery over Lukole refugee camp, Tanzania. *Int. J. Remote Sens* 24
622 (22), 4251-4266.

623 Gonsalves, A.D., 1955. O Babaçu, considerações científicas, técnicas e econômicas.
624 Ministério da Agricultura, Rio de Janeiro, Série Estudos e Ensaio n° 8, 321p.

625 Haralick, R.M., Stenberg S.R., Zhuang X., 1987. Image analysis using mathematical
626 morphology. *IEEE T Pattern Anal* PAMI-9(4), 532-550. DOI:
627 10.1109/TPAMI.1987.4767941.

628 Hirschmugl, M., Ofner, M., Raggam, J., Schardt, M., 2007. Single tree detection in very high
629 resolution remote sensing data. *Remote Sens Environ* 110, 533–544.

630 IBGE, 2013. *Produção da Extração vegetal e da silvicultura*. IBGE, Rio de Janeiro, v. 28, 69p.

631 Jiang, M., Lin, Y., 2013. Individual deciduous tree recognition in leaf-off aerial ultrahigh
632 spatial resolution remotely sensed imagery. *IEEE Geosci Remote Sens Lett.* 10, 38–42.

633 Johansen, K., Sohlbach, M., Sullivan, B., Stringer, S., Peasley, D., Phinn, S., 2014. Mapping
634 Banana Plants from High Spatial Resolution Orthophotos to Facilitate Plant Health
635 Assessment. *Remote Sensing* 6, 8261–8286. doi:10.3390/rs6098261.

636 Kahn, F., 1986. Adaptation en forêt tropicale humide: le cas des palmiers amazoniens. in:
637 Hallé, F. (ed.), *L'arbre: compte-rendu du colloque international*. *Naturalia Monspeliensia*,
638 Montpellier, p. 171-189.

639 Laurin, G.V., Chan, J.C.W., Chen, Q., Lindsell, J.A., Coomes, D.A., Guerriero, L., Frate, F.
640 D., Miglietta, F., Valentini, R., 2014. Biodiversity Mapping in a Tropical West African
641 Forest with Airborne Hyperspectral Data. *PLoS ONE* 9(6), e97910.
642 <http://dx.doi.org/10.1371/journal.pone.0097910>

643 Lin, M.J.Y., 2013. Individual Deciduous Tree Recognition in Leaf-Off Aerial Ultrahigh
644 Spatial Resolution Remotely Sensed Imagery. *IEEE Geosci Remote Sens Lett* 10(1), 38-
645 42.

646 Lorenzi, H., Noblick, L.R., Kahn, F., Ferreira, E., 2010. *Flora brasileira – Arecaceae*
647 (Palmeiras). *Plantarum*, São Paulo, 384 p.

648 Luo, L., Wang, X., Guo, H., Liu, C., Liu, J., Li, L., Du, X., Qian, G., 2014. Automated
649 Extraction of the Archaeological Tops of Qanat Shafts from VHR Imagery in Google
650 Earth. *Remote Sensing* 6(12), 11956-11976.

651 Malek, S., Bazi, Y., Alajlan, N., Alhichri, H., Melgani, F., 2014. Efficient Framework for
652 Palm Tree Detection in UAV Images. *IEEE J-STARS* 7(12), 4692-4703.

653 Martins, R.C., Filgueiras, T.S., Albuquerque, U.P., 2014. Use and Diversity of Palm
654 (Arecaceae) Resources in Central Western Brazil. The Scientific World Journal ID
655 942043, 14 pages. <http://dx.doi.org/10.1155/2014/942043>

656 May, P.H., Anderson, A.B., Balick, M.J., Frazão, J.M.F., 1985. Subsistence benefits from the
657 babassu palm (*Orbignya martiana*). Econ Bot 39,113-129.

658 Mitja, D., Miranda, I.S., Velasquez, E., Lavelle, P., 2008. Plant species richness and floristic
659 composition change along a rice-pasture sequence in subsistence farms of Brazilian
660 Amazon, influence on the fallows biodiversity (Benfica, State of Pará). Agr Ecosyst
661 Environ 124(2), 72-84.

662 Mitja, D., Ferraz, I., 2001. Establishment of babassu in pastures in Pará, Brazil. Palm
663 trees 45(3), 138-147.

664 Mitja, D., Miranda, I.S. 2010. Weed community dynamics in two pastures grown after
665 clearing Brazilian Amazonian rainforest. Weed Res 50, 163–173.

666 Montúfar, R., Anthelme, F., Pintaud, J.C., Balslev, H., 2011. Disturbance and Resilience in
667 Tropical American Palm Populations and Communities. The Botanical Review 77(4),
668 426-461.

669 Pintaud, J.-C., Galeano, G., Balslev, H., Bernal, R., Borschenius, F., Ferreira, E., Granville, J.
670 J., Mejía, K., Millán, B., Moraes, M., Noblick, L., Stauffer, F.W., Kahn, F., 2008. Las
671 palmeras de América del Sur: diversidad, distribución e historia evolutiva. Revista
672 Peruana de Biología 15(Supl. 1), 7–29.

673 Porro, N., Veiga, I., Mota, D., 2011. Traditional communities in the Brazilian Amazon and
674 the emergence of new political identities: the struggle of the quebradeiras de coco babaçu
675 - babassu breaker women. Journal of Cultural Geography 28 (1), 123-146.

676 Porro, R., Porro, N.S.M., 2014. Social roots of resource use routes in rural Maranhão, Brazil.
677 Journal of Rural Studies 36, 64-76.

678 Pouliot, D.A., King, D.J., Bell, F.W., Pitt, D.G., 2002. Automated tree crown detection and
679 delineation in high-resolution digital camera imagery of coniferous forest regeneration.
680 *Remote Sens Environ* 82, 322-334.

681 Protásio, T.P., Trugilho, P.F., César, A.A.S., Napoli, A., Melo, I.C.N.A., Silva, M.G., 2014.
682 Babassu nut residues: potential for bioenergy use in the North and Northeast of
683 Brazil. *SpringerPlus* 3 (1), 1. Doi:10.1186/2193-1801-3-124

684 R Core Team, 2014. R: a language and environment for statistical computing. R Foundation
685 for Statistical Computing. <http://www.R-project.org/> (accessed 14.01.17).

686 Rich, P.M., Helenurm, K., Kearns, D., Morse, S.R., Palmer, M.W., Short, L., 1986. Society
687 Height and Stem Diameter Relationships for Dicotyledonous Trees and Arborescent Palm
688 trees of Costa Rican Tropical Wet Forest. *B Torrey Bot Club* 113 (3), 241-246.

689 Ritter, L., Martins, P., Cooper, M., Grimaldi, C., 2009. Variação e possibilidades de uso do
690 solo sobre rochas cristalinas na Amazônia oriental. *Novos Cadernos NAEA* 12(1), 225-
691 246.

692 Sampaio, S.M.N., 2008. Dinâmica da paisagem e complexidade espacial de um Projeto de
693 Assentamento da Amazônia Oriental. 2008. Thesis (PhD), Universidade Federal Rural da
694 Amazônia. 175 p.

695 Santos, A.M., Mitja, D., 2011. Wooded cattle pasture in the benfica seetling project in
696 Itupiranga, Pará, Brazil. *Rev Arvore* 35(4), 919-930.

697 Schmidtlein, S., Feilhauer, H., Bruelheide, H., 2012. Mapping plant strategy types using
698 remote sensing. *J Veg Sci* 23, 395–405.

699 Serra, J., 1982. Image analysis and mathematical morphology. Academic Press, New-York.

700 Shafri, H.Z.M., Hamdan, N., Saripan, M.I., 2011. Semi-automatic detection and counting of
701 oil palm trees from high spatial resolution airborne imagery. *Int J Remote Sens* 32(8),
702 2095-2115. <http://dx.doi.org/10.1080/01431161003662928>

703 Shufelt, J.A., 1999. Performance evaluation and analysis of monocular building extraction
704 from Aerial imagery. *IEEE T Pattern Anal* 21, 311–326. DOI: 10.1109/34.761262

705 Soille, P., Pesaresi, M., 2002. Advances in mathematical morphology applied to geoscience
706 and remote sensing. *IEEE T Geosci Remote* 40, 2042–2055.

707 Srestasathiern, P., Rakwatin, P., 2014. Oil Palm Tree Detection with High Resolution Multi-
708 Spectral Satellite Imagery. *Remote Sensing* 6(10), 9749-9774.

709 Teixeira, M.A., 2003. Uma Agenda para o Babaçu. *Revista Econômica do Nordeste* 34(4),
710 562-575.

711 Torres-Méndez, L.A., Ruiz-Suárez, J.C., Sucar, L.E., Gómez, G., 2000. Translation Rotation
712 and Scale-Invariant Object Recognition. *IEEE T Systems Man and Cybernetics*, 30:125-
713 130. DOI: 10.1109/5326.827484.

714 Wang, Y.H., Augspurger, C., 2006. Comparison of seedling recruitment under arborescent
715 palm trees in two Neotropical forests. *Oecologia* 147(3), 533-45.

716 Whiteside, T., Boggs, G., Maier, S., 2011. Extraction of tree crowns from high resolution
717 imagery over Eucalypt dominant tropical savanna. *Photogramm Eng Rem S* 77 (8), 813-
718 824.

719 Zhang, J., Rivard, B., Sánchez-Azofeifa, A., Castro-Esau, K., 2006. Intra- and inter-class
720 spectral variability of tropical tree species at La Selva, Costa Rica: Implications for
721 species identification using HYDICE imagery. *Remote Sens Environ* 30 105(2), 129-141.
722 <http://dx.doi.org/10.1016/j.rse.2006.06.010>

723 Zhou, J., Proisy, C., Descombes, X., Le Maire, G., Nouvellon, Y., José-Luiz, S., Viennois, G.,
724 Zerubia, J., Couteron, P., 2013. Mapping local density of young Eucalyptus plantations
725 by individual tree detection in high spatial resolution satellite images. *Forest Ecol Manag*
726 301, 129-141. <http://dx.doi.org/10.1016/j.foreco.2012.10.007>